IEEE Access
Multidisciplinary | Rapid Review | Open Access Journal

Received May 18, 2019, accepted June 12, 2019, date of publication July 16, 2019, date of current version August 13, 2019.

Digital Object Identifier 10.1109/ACCESS.2019.2928968

Dynamic Behaviors and Protection Strategy of Synchronous Condenser Integrated Power System Under Non-Full Phase Fault Conditions

PUYU WANG[1], (Member, IEEE), XING LIU[1], QINGWEN MOU[1], WEI GU[2], (Senior Member, IEEE), AND YIDAN LIU[3]

[1]Department of Electrical Engineering, School of Automation, Nanjing University of Science & Technology, Nanjing 210094, China
[2]Jiangsu Provincial Key Laboratory of Smart Grid Technology & Equipment, Southeast University, Nanjing 210096, China
[3]Jiangsu Electric Power Maintenance Branch Company, Nanjing 211100, China

Corresponding author: Puyu Wang (puyu.wang@hotmail.com)

This work was supported in part by the National Natural Science Foundations of China under Grant 51807091, in part by the Natural Science Foundation of Jiangsu Province under Grant BK20180478, in part by the Fundamental Research Funds for the Central Universities under Grant 30917011330, and in part by the Science and Technology Program of the State Grid Jiangsu Electric Power Company Ltd., under Grant 5210EC16000Q.

ABSTRACT When a synchronous condenser connected power network encounters a non-full phase fault, the amplitude of the stator current is severely suppressed by the magnetic field generated inside the synchronous condenser, in which the sensitivity of failure protection of circuit breakers are affected resulting in rejection of failure protection. In severe cases, it may endanger the secure and stable operation of the synchronous condenser and the related equipment. In this paper, dynamic behaviors of a synchronous condenser without/with de-excitation action under non-full phase faults are investigated with the following four contributions: 1) A mathematical model under non-full phase fault conditions is established. The theoretical value of fault currents is calculated when the synchronous condenser is without/with de-excitation action. 2) The inferiority/superiority without/with de-excitation action is analyzed. The tendency of dynamic behaviors of variables, including the phase current, negative-sequence, and zero-sequence currents, after de-excitation action, is obtained. A selection criterion of failure protection is proposed according to the dynamic behaviors of negative- and zero-sequence currents. 3) Based on the consistent characteristics of the theoretical calculation, simulations in PSCAD/EMTDC and recorded on-site data from WaveEx, the fact that the simulation model established in PSCAD/EMTDC can provide an effective verification platform for practical applications and data analysis of a synchronous condenser integrated power grid under non-full phase faults is justified. 4) An improved operational threshold of failure protection of circuit breakers is proposed. It can reduce the rejection operation probability of failure protection, which improves the protection sensitivity and enhances the security of the system operation. The simulation results justify the necessity and reliability of the criterion setting proposed for failure protection.

INDEX TERMS Synchronous condenser, non-full phase fault, without/with de-excitation action, failure protection of circuit breakers, selection criterion, and operational threshold.

I. INTRODUCTION

With rapid development of AC/DC hybrid power network and the structure of high voltage direct current (HVDC) grid currently at a transition period, the operation of power grids is presenting new features with a variety of forms. Penetrations of renewable power resources, e.g. wind and solar energy, are increased significantly [1]–[3], which result in more challenges in reactive power control and voltage stability issues becoming more prominent. In addition, the operation of converter stations, particularly under disturbance or fault condition [4], requires rapid and sufficient reactive power support,

The associate editor coordinating the review of this manuscript and approving it for publication was Maddikara Jaya Bharata Reddy.

which brings higher requirements for reactive power compensation devices with large capacity and dynamic reactive power support. Currently, applications of dynamic reactive power compensation devices in ultra-HVDC (UHVDC) converter stations are mainly represented by rotating motor devices, e.g. synchronous condensers and power electronic devices, e.g. static var compensation (SVC) [5]. In comparison with the SVC, synchronous condensers have strong capability of overloading and can provides strong reactive power support under fault conditions in a short period. In addition, their reactive power outputs can be flexibly adjusted according to the needs of compensation and the operating conditions of power grids in real-time [6]. However, research has been rarely conducted regarding the fault behaviors of synchronous condenser under non-full phase faults without/with de-excitation operation.

When a non-full phase fault occurs on the system side, the current output of the synchronous condenser is suppressed due to the rotating magnetic field generated by the stator windings and the rotor magnetic field generated by the rotor windings [7]. This results in the consequence that amplitude of negative- and zero-sequence currents cannot reach the operational threshold of relay protection and thus lead to the tripping failure of circuit breakers. Hence, the sensitivity of the failure protection is reduced. Generally, no overcurrent or overvoltage emerges under non-full phase faults in power systems. However, the negative-sequence current generated under non-full phase fault may result in damages on the stator and rotor of synchronous condensers. In addition, the zero-sequence current will have interference on adjacent communication lines. Meanwhile, either the negative- or zero-sequence current may result in mal-operation of relay protection [8], [9]. The eddy current loss on the rotor surface induced by the negative-sequence current was analyzed in [10] when the non-full phase fault occurred on the high-voltage side of the transformer. The results indicated that the transient eddy current loss was more significant under a two-phase non-full phase fault than that under a single-phase non-full phase fault. The dynamic behaviors of grid integration of synchronous condensers with different frequencies and variable-slip modes were investigated in [11]. The grid integration instant under the worst condition was calculated. An optimized grid integration frequency was proposed. However, precise control sequences of the synchronous condenser with variable-frequency control was not discussed. The behaviors of the output voltages and currents of a generator under single-and two-phase non-full phase faults on the high-voltage side of the main transformer were studied in [12]. The results indicated that the rotor would not been damaged when the negative-sequence current did not exceed the secure threshold. However, the impact of sequence currents on the sensitivity of failure protection was not analyzed under non-full phase faults. In [13], the eddy current loss and rise of temperature were calculated due to negative-sequence current generated on the rotor surface under the asymmetric fault. However, the characteristics of zero-sequence current was not analyzed. According to aforementioned literature, research has been conducted regarding theoretical analysis, calculations and dynamic behaviors of conventional generators under non-full phase fault conditions, while there has been few study regarding the synchronous condenser integrated power system under non-full phase fault conditions. In addition, no research has been carried out regarding synchronous condensers without/with de-excitation action after non-full phase faults on the system side, which significantly affected the response and sensitivity of failure protection.

In this paper, topological structure of a voltage-sourced converter (VSC)-based static frequency converter (SFC) integrated synchronous condenser is developed. After that, precise control sequences of the synchronous condenser without/with de-excitation action are proposed. Fault behaviors of the synchronous condenser under non-full phase faults without/with de-excitation action are studied. In addition, a mathematical model under the fault conditions is established. Theoretical values of fault currents are calculated without/with de-excitation action. Dynamic behaviors of the fault currents and sensitivity of relay protection under the non-full phase faults are analyzed with discussions of the inferiority/superiority without/with de-excitation action. The tendency of the system dynamic behaviors, including the phase current, negative- and zero-sequence currents, with de-excitation action is obtained. A criterion of operational threshold of failure protection is proposed according to the dynamic behaviors of the negative- and zero-sequence currents. In addition, an operational threshold of failure protection is proposed. It can reduce the rejecting operation probability of failure protection, which improves the protection sensitivity and enhances the security of the systems operation. The simulation model established in PSCAD/EMTDC can provide an effective verification platform for practical applications and data analysis of a synchronous condenser integrated power grid under non-full phase faults.

II. TOPOLOGICAL STRUCTURE AND CONTROL SEQUENCE OF AN SFC INTEGRATED SYNCHRONOUS CONDENSER

A. TOPOLOGICAL STRUCTURE

In order to study the dynamic behaviors of a synchronous condenser under non-full phase faults on the high-voltage side of the main transformer, a simulation system of a 300 MVar synchronous condenser with VSC-based SFC is established in the time-domain simulation software PSCAD/EMTDC. The diagram of the topological structure of the system is illustrated in Fig. 1. The SFC is depicted in the blue dotted-line frame. It comprises a three-phase six-bridge DC/AC inverter, which consists of VSC-based insulated-gate bipolar transistors (IGBTs) and a DC power supply. The synchronous condenser, including the excitation part and synchronous motor, is connected to the SFC via SFC circuit breaker (CB_SFC). The AC grid connects to the synchronous

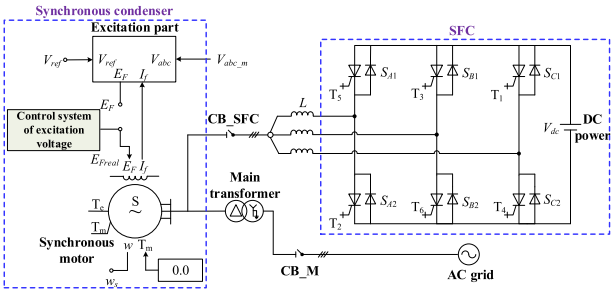

FIGURE 1. Schematic diagram of the synchronous condenser interconnected AC grid with SFC.

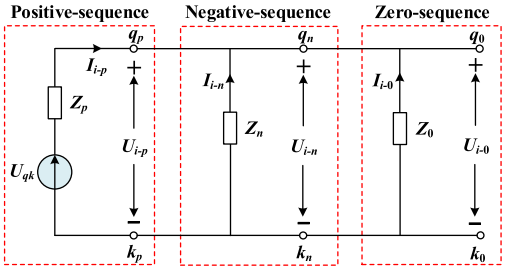

FIGURE 2. The composite network of a single-phase open-circuit fault.

condenser via the main transformer and the main circuit breaker (CB_M), i.e. the integration circuit breaker.

B. CONTROL SEQUENCE

The synchronous condenser is initiated by the variable-frequency control mode. Initially, the rotor speed increases with the growth of the frequency of the condenser terminal voltage. When the rotor speed reaches 105% of the rated speed, CB_SFC is disconnected, i.e. the SFC is disconnected from the synchronous condenser. Then, the synchronous condenser moves into the speed-falling operation mode. The control sequences of start-up and grid-integration of the synchronous condenser is explained as follows.

- **Step 0:** Initially, the synchronous condenser is in static mode and the SFC is blocked;
- **Step 1:** The VSC-based SFC is deblocked to control the SFC AC-side voltage;
- **Step 2:** The excitation part is activated and the CB_SFC is connected;
- **Step 3:** The variable-frequency control is activated and applied on the SFC to gradually increase the frequency of the condenser output voltage. When the rotor speed rises to the pre-set value, i.e. 105% of the nominal speed, CB_SFC is disconnected;
- **Step 4:** The synchronous condenser moves to the speed-falling operation mode, where the stator voltage is established at this stage. When the constraint criterions of grid-synchronization are satisfied, CB_M is closed for the completion of the integration process.

III. MODELLING AND ANALYSIS OF SYNCHRONOUS CONDENSER UNDER NON-FULL PHASE FAULTS

In this section, a mathematical model, precise control sequences of the condenser without/with de-excitation action, and dynamic behaviors of the synchronous condenser under non-full phase fault are analyzed. Power units and transmission lines should be equipped with main protection and backup protection. The backup protection should be rapidly activated to remove the fault when the main protection fails to operate, e.g. mal-operation/rejecting action of circuit breakers [14]. Failure protection of circuit breakers are generally utilized under such conditions to achieve fault removal. It is an important backup protection in relay protection, which has direct impact on the secure and stable operation of power systems [15]. In order to discriminate failures of the main protection, the information of protection actions and currents of the faulted equipment are taken by the device of failure protection [16]. Then the fault is rapidly removed by the failure protection within a short period and the range of power outages is limited to the lowest level. This ensures stable operation of the overall power grid and avoids damages on the synchronous condenser and the related units.

A. MATHEMATICAL MODEL OF NON-FULL PHASE FAULT CONDITIONS

Under non-full phase fault conditions, vertical-asymmetric condition emerges at the open-circuit location, while the rest part of the system maintains symmetrical operation, which is denoted as vertical-asymmetric fault [17]. Similar to asymmetric short-circuit faults, i.e. horizontal-asymmetric faults, the symmetrical component method can be utilized to analyze the mathematical relationship of non-full phase fault conditions [18].

1) A SINGLE-PHASE OPEN-CIRCUIT FAULT

The boundary condition of a single-phase open-circuit fault is the same as that of a two-phase short-circuit grounded fault. Thus, the boundary conditions can be derived by applying the symmetrical component method as

$$\begin{cases} \dot{I}_{i-p} + \dot{I}_{i-n} + \dot{I}_{i-0} = 0 \\ \dot{U}_{i-p} = \dot{U}_{i-n} = \dot{U}_{i-0} \end{cases} \tag{1}$$

where, $\dot{I}_{i-p}, \dot{I}_{i-n}, \dot{I}_{i-0}$ $(i = a, b, c)$ are positive-, negative-, and zero-sequence current components on the Y-side of the transformer, respectively. $\dot{U}_{i-p}, \dot{U}_{i-n}, \dot{U}_{i-0}$ are positive-, negative- and zero-sequence voltage components on the Y-side of the transformer, respectively. According to the boundary condition presented in (1), the composite sequence network is depicted in Fig. 2.

In Fig. 2, q_u and k_u $(u = p, n, 0)$ are the fault points at the open-ports, respectively.

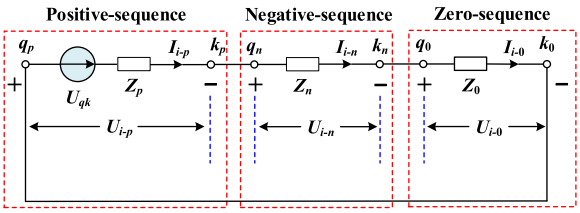

FIGURE 3. The composite network of a two-phase open-circuit fault.

The positive-, negative- and zero-sequence components of the currents under the single-phase open-circuit fault are derived as

$$\begin{cases} \dot{I}_{i-p} = \dfrac{\dot{U}_{qk}}{Z_p + Z_n \parallel Z_0} \\ \dot{I}_{i-n} = -\dfrac{Z_0}{Z_n + Z_0}\dot{I}_{i-p} \\ \dot{I}_{i-0} = -\dfrac{Z_n}{Z_n + Z_0}\dot{I}_{i-p} \end{cases} \tag{2}$$

where, U_{qk} is the voltage between port q-k when the port is open. Z_p, Z_n, Z_0 are the equivalent impedances of positive-, negative- and zero-sequence networks from port q-k, respectively.

The currents of the non-fault phases are calculated as

$$\dot{I}_j = \left(\alpha^2 - \frac{Z_n + \alpha Z_0}{Z_n + Z_0}\right)\dot{I}_{i-p}$$
$$\dot{I}_k = \left(\alpha - \frac{Z_n + \alpha^2 Z_0}{Z_n + Z_0}\right)\dot{I}_{i-p} \tag{3}$$

$$I_j = I_k = \sqrt{3} \times \sqrt{1 - \frac{Z_n \times Z_0}{(Z_n + Z_0)^2}}\, I_{i-p} \tag{4}$$

where, $\dot{I}_j$ and $\dot{I}_k$ are the currents of the non-fault phases on the Y-side of the transformer, respectively.

2) TWO-PHASE OPEN-CIRCUIT FAULT

The boundary condition of a two-phase open-circuit fault is the same as that of a single-phase short-circuit grounded fault. Thus, the boundary conditions can be derived as

$$\begin{cases} \dot{I}_{i-p} = \dot{I}_{i-n} = \dot{I}_{i-0} \\ \dot{U}_{i-p} + \dot{U}_{i-n} + \dot{U}_{i-0} = 0 \end{cases} \tag{5}$$

According to (5), the composite sequence network is illustrated in Fig. 3.

The sequence current components of two-phase open-circuit fault are proposed as

$$\dot{I}_{i-p} = \dot{I}_{i-n} = \dot{I}_{i-0} = \frac{\dot{U}_{qk}}{Z_p + Z_n + Z_0} \tag{6}$$

The non-fault phase current is expressed as

$$\dot{I}_i = 3\dot{I}_{i-p} = \frac{3\dot{U}_{qk}}{Z_p + Z_n + Z_0} \tag{7}$$

B. PRECISE CONTROL SEQUENCES OF SYNCHRONOUS CONDENSER WITHOUT/WITH DE-EXCITATION ACTION

A non-full phase fault is a special case in asymmetric faults and is considered as a serious fault condition. If the non-full phase fault is not detected due to improper settings of protection thresholds and the synchronous condenser does not activate relay protection actions, it may result in damages on the synchronous condenser and the related units. In addition, considering the fact that a synchronous condenser with large capacity is expensive, huge economic losses may occur after non-full phase faults if proper protection threshold is not applied. In this paper, dynamic behaviors of a synchronous condenser without/with de-excitation action under non-full phase faults are investigated. Precise control sequences of the synchronous condenser without/with de-excitation action are proposed as follows.

(1) Without de-excitation action

The precise control sequences without de-excitation under phase A (or phase AB) non-full phase fault are described as follows.

•**Step 1:** Initially, the synchronous condenser is under steady-state operating conditions;

•**Step 2:** The circuit breaker of phase A (or phase AB) is tripped to mimic a non-full phase fault condition;

•**Step 3:** The output currents of the synchronous condenser and the currents of the high voltage of main transformer, and their sequence components are recorded.

(2) With de-excitation action

The precise control sequences with de-excitation action under phase A (or phase AB) non-full phase fault are described as follows.

•**Step 1** and **Step 2** are the same as those of the previous case without de-excitation action;

•**Step 3:** The de-excitation circuit breaker is initiated, i.e. the de-excitation circuit breaker, which interconnects the excitation voltage generated from the excitation system with the excitation input of the synchronous condenser, is tripped, resulting in excitation voltage ($E_F = 0$) becomes zero;

•**Step 4** is the same as that of the previous case without de-excitation action.

Generally, a rotating magnetic field in the form of reversed synchronization may be generated between the air gap of the stator and rotor when negative-sequence currents flow through the synchronous condenser. Meanwhile, the rotor is rotating in accordance with the synchronous magnetic field, which leads to the result that the rotor has twice of the synchronous speed with respect to the rotating magnetic field in the form of reversed synchronization. This will result in currents with doubling frequency induced on the rotor surface, leading to rise of rotor temperature. In severe cases, it may result in significant damages of the related units [19].

The synchronous condenser with de-excitation action is beneficial to eliminating the magnetic field induced on the rotor surface, which increases the current amplitude. The information of the current can be utilized by the failure protection device to discriminate failures of the

TABLE 1. Negative-sequence & zero-sequence currents under a single-phase non-full phase fault.

Sequence current	Without de-excitation			With de-excitation		
	Theoretical calculation	PSCAD simulation	WaveEx data	Theoretical calculation	PSCAD simulation	WaveEx data
Negative-sequence current at the machine-end (A)	125	120	129	1625	1545	1512
Zero-sequence current at the machine-end (A)	0	0	1	0	0	12
Negative-sequence current at the high-voltage side (A)	5	5	5	65	62	58
Zero-sequence current at the high-voltage side (A)	10	11	9	123	146	116

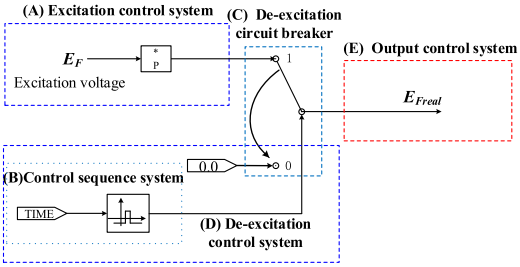

FIGURE 4. A schematic diagram of the control of the excitation voltage and de-excitation action.

circuit breaker. Thus, the fault may be instantly removed by the effective action of failure protection. The sensitivity and reliability of failure protection is improved owing to the increase of the current amplitude due to the de-excitation action. The event of grids collapse due to refusals of failure protection leading to continuous tripping of subsequent systems is thus avoided. In addition, the de-excitation action can eliminate the eddy current loss induced by the negative-sequence current on the rotor surface. Thus, the insulation loss is avoided and the service life of electrical equipment is increased. The control of the de-excitation action is proposed in this paper. A schematic diagram of the control of the excitation voltage and de-excitation action is illustrated in Fig. 4.

Under normal operating conditions, the tap of de-excitation circuit breaker is placed at 1 and the output voltage is E_F. When the de-excitation action is initiated, the control sequence system will send commands changing the tap of de-excitation circuit breaker to 0 and the output voltage becomes 0. Thus, the de-excitation control is executed.

C. OPERATING BEHAVIORS UNDER SINGLE-PHASE NON-FULL PHASE FAULT

When the synchronous condenser operates with no-load condition, the amplitude of negative- and zero-sequence currents on the machine-end and the high-voltage side of main transformer under a single-phase open-circuit fault are presented in Table 1. The data from WaveEx is the sequence currents of a synchronous condenser, which was recorded on-site in a real project with experiments, operating with no-load condition under a single-phase non-full phase fault.

Table 1 demonstrates that the simulation results from PSCAD are closed to the theoretical calculation and WaveEx data within allowable errors. The zero-sequence current at the machine-end is zero in the theoretical calculation and PSCAD, since the main transformer is in Y/Δ connection, in which the zero-sequence current forms a loop in the delta side and cannot flow out of the transformer windings. The zero-sequence current at the machine-end recorded in WaveEx is very small but not zero, which is acceptable in practical engineering, due to various uncertainty issues in real applications. Table 1 shows that the negative-sequence current at the machine-end and the zero-sequence current at the high-voltage side of main transformer increase significantly when the de-excitation action is conducted after the fault. In theoretical calculation, the amplitude of the negative-sequence current increases from 125 A to 1625 A, i.e. 12 times of increase. In PSCAD and WaveEx, the amplitudes of the negative-sequence currents have increases over 11 times with the de-excitation action. In addition, the amplitudes of zero-sequence currents at the high-voltage side have similar increases of 11.3 times, 12.3 times and 12 times, in theoretical calculation, PSCAD and WaveEx after the de-excitation action.

In Table 1, regarding the negative- and zero-sequence currents at the machine-end, the former one has more significant increase after the de-excitation action and is over 1000 A. However, for the negative- and zero-sequence currents at the high-voltage side, the latter one increases over 100 A with de-excitation action. Hence, considering the operational thresholds of failure protection, the negative-sequence current at the machine-end is selected as the operational threshold of failure protection, while the zero-sequence current at the high-voltage side of main transformer is selected as the operational threshold of failure protection.

D. OPERATING BEHAVIORS UNDER TWO-PHASE NON-FULL PHASE FAULT

When the synchronous condenser operates with no-load condition, the amplitude of negative- and zero-sequence currents on the machine-end and the high-voltage side of main transformer under a two-phase open-circuit fault are presented in Table 2. The data from WaveEx was recorded on-site in a real project with experiments under a two-phase non-full phase fault.

Table 2 shows that the simulation results from PSCAD are closed to the theoretical calculation and WaveEx data within allowable errors. The negative-sequence at the machine-end and the sequence currents at the high-voltage side have more

TABLE 2. Negative-sequence & zero-sequence currents under a two-phase non-full phase fault.

Sequence current	Without de-excitation			With de-excitation		
	Theoretical calculation	PSCAD simulation	WaveEx data	Theoretical calculation	PSCAD simulation	WaveEx data
Negative-sequence current at the machine-end (A)	250	280	264	4275	4527	4123
Zero-sequence current at the machine-end (A)	0	0	0	0	0	13
Negative-sequence current at the high-voltage side (A)	10	9	10	171	178	166
Zero-sequence current at the high-voltage side (A)	10	9	10	171	178	166

significant increase when the de-excitation is conducted after the fault. In theoretical calculation, the amplitude of the negative-sequence current increases from 250 A to 4275 A, which is about 17 times. In PSCAD and WaveEx, the amplitudes of the negative-sequence currents have augments around 15 times with the de-excitation action. In addition, in theoretical calculation, the amplitude of negative- and zero-sequence currents at the high-voltage side increases from 10 A to 171 A with around 16 times. The amplitudes of sequence currents at the high-voltage side have similar increases of 19 times, around 19 times, in PSCAD and WaveEx after the de-excitation action. The operational threshold of failure protection is more easily triggered and initiated when the amplitude of sequence current have more significant change.

In Table 2, regarding the negative- and zero-sequence currents at the machine-end, the former one has more significant increase after the de-excitation action and is over 4000 A. However, for the negative- and zero-sequence currents at the high-voltage side and those is the same. Hence, considering the operational thresholds of failure protection, the negative-sequence current at the machine-end is selected as the operational threshold of failure protection, while the negative- or zero-sequence currents at the high-voltage side are selected as the operational threshold of failure protection.

The results in Table 1 and Table 2 show that the sequence currents in PSCAD and WaveEx are very close under single- and two-phase non-full phase faults. Hence, the simulation model established in PSCAD is effective and can be utilized as a reliable verification platform in practical applications. In order to select an appropriate operational threshold of failure protection and improve the protection sensitivity, dynamic behaviors of the phase current, negative- and zero-sequence currents, are analyzed in Section IV based on the established simulation model in PSCAD.

IV. DYNAMIC BEHAVIORS OF THE SYNCHRONOUS CONDENSER UNDER NON-FULL PHASE FAULTS

In this section, dynamic behaviors of the currents at the machine-end and high-voltage side are analyzed without/with the de-excitation action under non-full phase faults.

A. SINGLE-PHASE NON-FULL PHASE FAULT

1) DYNAMICS OF THE PHASE CURRENTS

Initially, the synchronous condenser is started with the SFC. The synchronization control is activated to capture the synchronization grid connection point when the grid constraint criterions are met and then the synchronous condenser gradually performs the steady state operating condition [20]. When a vertical fault occurs, e.g. when a single-phase to ground fault occurs, the circuit breakers at both ends of the faulted line are tripped to isolate the fault, it may result in the system changing to deficient phase operation. This seriously affects the secure and stable operation of the synchronous condenser and related units. Fig. 5 demonstrates one phase current of the synchronous condenser under a single-phase non-full phase fault at 10 s at the high-voltage side of the main transformer.

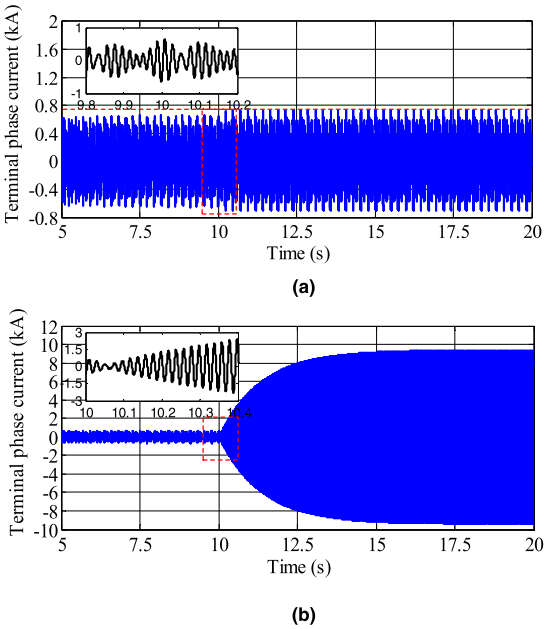

FIGURE 5. Phase current of the synchronous condenser under a single-phase non-full phase fault. (a) Without de-excitation. (b) With de-excitation.

Fig. 5 (a) shows that the amplitude of the phase current has slight increase after the fault and the amplitude of fluctuations is within [-0.8 kA, 0.8 kA] when the synchronous condenser is without de-excitation action. Fig. 5 (b) shows that the phase current increases rapidly after the fault when the de-excitation action is applied. The amplitude of the phase current increases from 0.6 kA to 9.4 kA, which is augmented over 15 times. The results demonstrate that the amplitude of the phase current with de-excitation action increases significantly in comparison with that without de-excitation action.

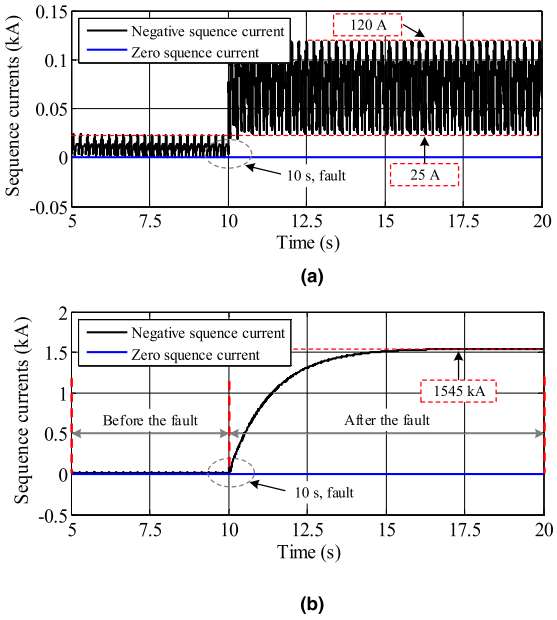

FIGURE 6. Sequence current components of the phase currents. (a) Without de-excitation. (b) With de-excitation.

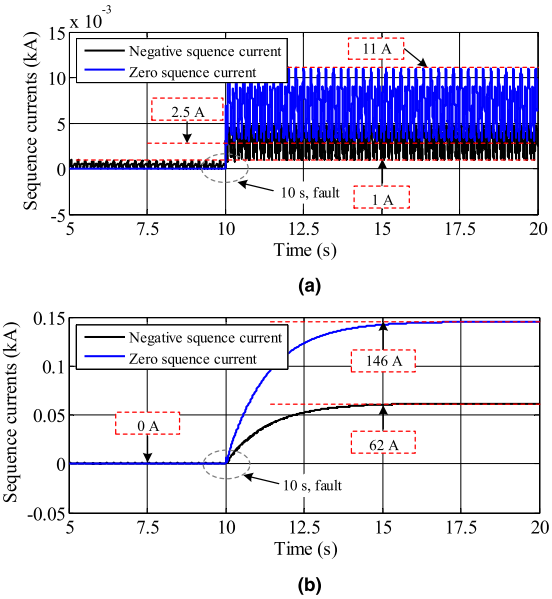

FIGURE 7. Sequence current components of the phase currents. (a) Without de-excitation. (b) With de-excitation.

2) DYNAMICS OF SEQUENCE CURRENT COMPONENTS AT THE MACHINE-END

Fig. 6 shows the sequence current components of the phase currents at the machine-end.

Fig. 6 (a) shows that the amplitude of the negative-sequence current is initially within the range of [0, 25 A] and increases to the range of [25 A, 120 A] after the fault. If the operational threshold of failure protection is set to 100 A, when a non-full phase fault occurs, the highest amplitude of the negative-sequence current will exceed the operational threshold activating the failure protection. Hence, the failure protection of circuit breakers will achieve the fault removal when the main circuit breaker of relay protection encounters rejecting operation. If the operational threshold of failure protection is set to 200 A, the highest amplitude of the negative-sequence current is less than the operational threshold when a non-full phase fault occurs resulting in rejecting operation of failure protection. Refusal of failure protection may further lead to continuous tripping of the subsequent system, which may result in collapse of the power grids. Fig. 6 (b) shows that the amplitude of the negative-sequence current increases rapidly to over 1.5 kA after the fault with de-excitation action. The amplitude is augmented by 11.5 times, which is beneficial to for the failure protection to detect the incident and activate the tripping action. When the operational threshold of failure protection is set to 100 A or 200 A, the fault can both be effectively detected and removed by failure protection. Hence, when the operational threshold of failure protection is set to 100 A, the non-full phase fault can be effectively detected and removed regardless of the fact that the synchronous condenser is without/with the de-excitation action. Fig. 6 shows that the zero-sequence current is always zero before and after the fault due to delta connection on the low-voltage side. Hence, the zero-sequence current is not suggested as the indicator for failure protection.

3) DYNAMICS OF SEQUENCE CURRENT COMPONENTS AT THE HIGH-VOLTAGE SIDE

Fig. 7 shows the sequence current components of the phase currents at the high-voltage side.

Fig. 7 (a) shows that the amplitude of the negative-sequence current at the high-voltage side is within the range of [0, 5 A] and the zero-sequence current fluctuates within [2.5 A, 11 A] after the fault. The amplitudes of the sequence currents are small and cannot initiate the failure protection. Fig. 7 (b) shows that the amplitude of the negative-sequence current increases to over 60 A, which is not large enough to activate failure protection. However, the amplitude of the zero-sequence current at the high-voltage side increases significantly after 10 s due to the de-excitation action and reaches 146 A. If the operational threshold of failure protection is set to 100 A, the amplitude of the zero-sequence current exceeds the operational threshold, i.e. failure protection can be activated after the fault within 2 s. The fault is then removed and the reliability of failure protection is effectively improved. With the de-excitation action, failure protection is successfully activated and the activation period is sufficiently short. Thus, the fault can be removed rapidly, thereby ensuring the security of the synchronous condenser and the related power equipment.

4) DISCUSSION OF THE CURRENT DYNAMICS UNDER A SINGLE-PHASE NON-FULL PHASE FAULT

When a single-phase non-full phase fault occurs on the high-voltage side of the main transformer with de-excitation action applied at the synchronous condenser, the amplitude of the negative-sequence current at the machine-end has more

increase compared with that of the zero-sequence current, as shown in Fig. 6. However, the zero-sequence current at the high-voltage side has more increase compared with that of the negative-sequence current, as shown in Fig. 7. The increase of the current amplitude make failure protection effectively reach the operational threshold and can shorten the respond of failure protection. The sensitivity of failure protection is improved by setting an appropriate operational threshold. Initially, the current transformer (CT) ratio of the synchronous condenser is set as 2000:1, resulting in the operational threshold of failure protection being $0.1 \cdot I_{N1}$, i.e. 200 A. In the on-site applications, in order to enhance the sensitivity of failure protection, the CT ratio is changed to 1000:1, resulting in the operational threshold of failure protection becoming 100 A. According to the analysis and simulation results presented in Sections 3 & 4, failure protection at the machine-end can be activated when the operational threshold maintains 200 A, while failure protection at the high-voltage side cannot be activated. When the operational threshold is changed to 100 A, failure protection at both locations can be effectively activated. The sensitivity of failure protection is largely improved by adjusting the operational threshold and the simulation results justify the necessity of varying the CT ratio.

B. TWO-PHASE NON-FULL PHASE FAULT

1) DYNAMICS OF SEQUENCE CURRENT COMPONENTS AT THE MACHINE-END

The amplitudes of the sequence current opponents have more significant increase with the de-excitation action. The setting an operational threshold of failure protection is essential and can impact on the sensitivity of relay protection. When the operational threshold is set too large compared with operational threshold at 100 A, and that cannot be reached result in the sensitivity falling, which enables the system deficient phase operation. Hence, it is essential to select an appropriate the operational threshold so as to improve the sensitivity of failure protection. Fig. 8 shows the sequence current components of the phase currents at the machine-end.

Fig. 8 (a) shows that the amplitude of the negative-sequence current is initially 23 A and increases to the range of [110 A, 280 A] after the fault with a peak of 280 A. The amplitude of sequence current are large than the operational threshold, the failure protection at the machine-end is activated. In addition, the amplitude of the zero-sequence current keeps constant at 0 before and after the fault. Fig. 8 (b) shows that the synchronous condenser operates in full loss of-excitation state after the de-excitation action. The amplitude of the negative-sequence current increases significantly to a peak of over 4.5 kA after the fault. In comparison with the operational threshold at 200 A, the respond of failure protection can be shortened when the operational threshold is set 100 A. The sensitivity of failure

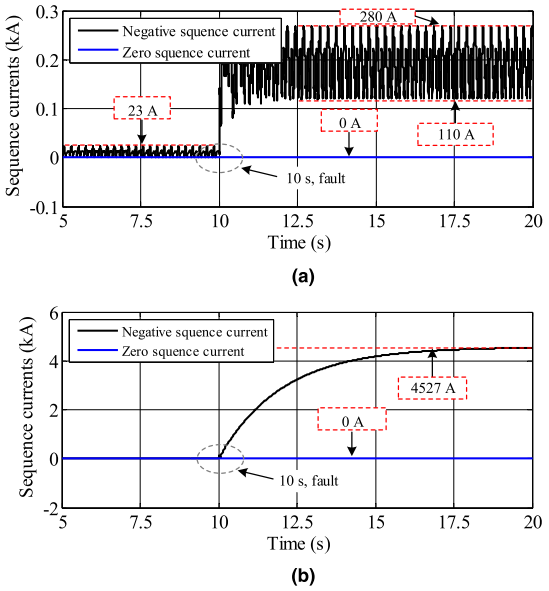

FIGURE 8. Sequence current components of the phase currents. (a) Without de-excitation. (b) With de-excitation.

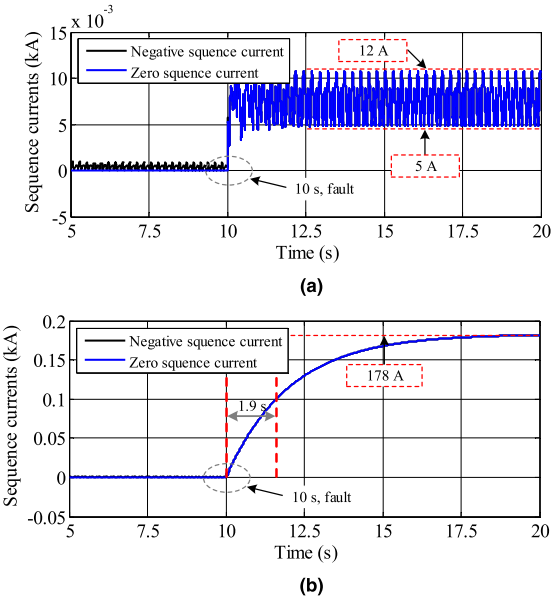

FIGURE 9. Sequence current components of the phase currents. (a) Without de-excitation. (b) With de-excitation.

protection is improved by setting an appropriate operational threshold.

2) DYNAMICS OF SEQUENCE CURRENT COMPONENTS AT THE HIGH-VOLTAGE SIDE

Fig. 9 shows the sequence current components of the phase currents at the high-voltage side.

Fig. 9 (a) shows that the amplitudes of negative- and zero-sequence currents are initially around 0 and increase to the range of [5 A, 12 A] after the fault and the same.

TABLE 3. Reliability of activating failure protection under a single-phase non-full phase fault.

	Without de-excitation	With de-excitation
Machine-end	success	success
The high-voltage side	fail	success

TABLE 4. Reliability of activating failure protection under a two-phase non-full phase Fault.

	Without de-excitation	With de-excitation
Machine-end	success	success
The high-voltage side	fail	success

The amplitudes of sequence currents are smaller than the operational threshold of failure protection and cannot initiate the failure protection. Fig. 9 (b) shows that the amplitudes of negative- and zero-sequence currents are the same and increase from 0 A to around 180 A. In order to enhance the sensitivity of failure protection, the operational threshold of protection criterion will be set as 100 A. It makes the amplitude of the sequence current reach the operational threshold more quickly, i.e. failure protection can be activated after the fault within 2 s, which can shorten the respond of failure protection.

3) DISCUSSION OF THE CURRENT DYNAMICS UNDER A TWO-PHASE NON-FULL PHASE FAULT

When a single-phase non-full phase fault occurs at the high-voltage side of the main transformer with de-excitation action applied, the amplitude of the negative-sequence current at the machine-end has more significant increase compared with that of the zero-sequence current, as shown in Fig. 8. However, the negative- and zero-sequence currents at the high-voltage side has more increase, as shown in Fig. 9. The increase of the current amplitude make failure protection effectively reach the operational threshold and can shorten the respond of failure protection. By discriminating failures of the main protection, the information of protection action and sequence currents of the faulted equipment are taken by the device of failure protection and then the fault is rapidly removed when the main circuit breaker of relay protection encounters rejecting operation. The simulation results are consistent with the selection of sequence current components as the criterion of operational threshold of failure protection in practical applications.

V. ANALYSIS AND DISCUSSION

The theoretical analysis and simulation results in Sections III-A & III-B indicate that the amplitudes of the currents increase significantly after the de-excitation action under non-full phase faults. The reliability of activating failure protection under a single-phase & two-phase non-full phase faults with operational threshold at 100 A are illustrated in Table 3 & Table 4, respectively.

TABLE 5. Reliability of activating failure protection under a single-phase non-full phase fault.

	Without de-excitation	With de-excitation
Machine-end	fail	success
The high-voltage side	fail	fail

TABLE 6. Reliability of activating failure protection under a two-phase non-full phase fault.

	Without de-excitation	With de-excitation
Machine-end	success	success
The high-voltage side	fail	fail

Table 3 & Table 4 show that without de-excitation action, failure protection at the machine-end can be activated successfully, while failure protection at the high-voltage side cannot be activated. With de-excitation action, the operational threshold at the machine-end and the high-voltage side can both be reached to initiate the failure protection. Hence, the reliability of failure protection with de-excitation action is improved. Under both fault conditions, it has a successful rate of 75% of activating failure protection with the operational threshold at 100 A. When the operational threshold is set to 200 A, the reliability of activating failure protection under a single-phase & two-phase non-full phase faults is presented in Table 5 & Table 6, respectively.

Table 5 shows that without the de-excitation action, failure protection at the machine-end and the high-voltage side both fails. With the de-excitation action, failure protection at the machine-end is activated successfully, while at the high-voltage side still fails. Hence, it only has a successful rate of 25% of activating failure protection, which is much lower compared with that with operational threshold at 100 A. Table 6 shows that without/with de-excitation, the operational threshold at the machine-end can both be reached to initiate the failure protection, while failure protection at the high-voltage side cannot be activated. Hence, it only has a successful rate of 50% of activating failure protection with the operational threshold at 200 A, which is lower compared with that with operational threshold at 100 A.

Synthesizing the above analysis, the reliability of activating failure protection can be improved by the de-excitation action and appropriate selecting the operational threshold.

VI. CONCLUSION

In this paper, the dynamic behaviors of a synchronous condenser without/with de-excitation action under non-full phase faults at high-voltage side of the main transformer are investigated. The topological structure and control sequence of an SFC integrated synchronous condenser have been explained. A mathematical model of non-full phase fault conditions has been established and precise control sequences of the

synchronous condenser without/with de-excitation action have been proposed. The operating behaviors of the synchronous condenser, particularly the sequence current components, under non-full phase faults have been analyzed with comparisons of the results from theoretical calculation, PSCAD simulation and on-site WaveEx data. With de-excitation action, the amplitude of sequence current components can be largely increased after faults. The tendency of dynamic behaviors of the phase current, sequence current components at the machine-end and high-voltage side without/with de-excitation action has been analyzed. A selection criterion of failure protection has been proposed according to the dynamic behaviors of negative- and zero-sequence currents. At the machine-end, the negative-sequence current has been selected, while at the high-voltage side of the main transformer, the zero-sequence current has been selected, as the operational thresholds of failure protection, respectively. The CT ratio has been varied from X_1:1 to X_2:1 and the operational threshold of failure protection has thus been adjusted to $0.1 \cdot I_{N2}$. The improved operational threshold of failure protection has been proposed to enhance the reliability of activating failure protection. The simulation results have justified the necessity and reliability of the criterion setting proposed for failure protection. The successful rate of activating failure protection can be significantly increased with appropriate selection of operational threshold and de-excitation action, and the respond speed of failure protection can be greatly shortened. The simulation model established in PSCAD/EMTDC can provide an effective verification platform for practical applications and data analysis of a synchronous condenser integrated power grid under non-full phase faults.

REFERENCES

[1] Y. Xue, X. P. Zhang, and C. H. Yang, "Commutation failure elimination of LCC HVDC systems using Thyristor-based controllable capacitors," *IEEE Trans. Power Del.*, vol. 33, no. 3, pp. 1448–1458, Jun. 2018.
[2] Y. Li, Y. Zhang, J. Song, L. Zeng, and J. Zhang, "A novel pilot protection scheme for LCC-HVDC transmission lines based on smoothing-reactor voltage," *Electric Power Syst. Res.*, vol. 168, pp. 261–268, Mar. 2019.
[3] S. Gao, Q. Liu, and G.-B. Song, "Current differential protection principle of HVDC transmission system," *IET Gener., Transmiss. Distrib.*, vol. 11, no. 5, pp. 1286–1292, Mar. 2017.
[4] S. S. Kalsi, D. Madura, and M. Ingram, "Superconductor synchronous condenser for reactive power support in an electric grid," *IEEE Trans. Appl. Supercond.*, vol. 15, no. 2, pp. 2146–2149, Jun. 2005.
[5] S. Teleke, T. Abdulahovic, T. Thiringer, and J. Svensson, "Dynamic performance comparison of synchronous condenser and SVC," *IEEE Trans. Power Del.*, vol. 23, no. 3, pp. 1606–1612, Jul. 2008.
[6] Y. Zhang and A. M. Gole, "Comparison of the transient performance of STATCOM and Synchronous condenser at HVDC converter stations," in *Proc. 11th IET Int. Conf. AC DC Power Transmiss.*, Jul. 2015, pp. 1–7.
[7] X. L. Cao, B. Y. Li, Y. H. Shen, H. L. Chen, J. L. Lu, and Y. D. Liu, "Electrical characteristics of generator transformer high voltage side on open phase operation and its effect on protection," *Power Syst. Prot. Cont.*, vol. 42, no. 15, pp. 34–38, Jul. 2014.
[8] X. Chen, J. Fu, Z. Fan, and Z. Xu, "Action features analysis on zero-sequence directional protection of line open phase running and sound phase grounding," *Power Syst. Prot. Cont.*, vol. 41, no. 6, pp. 82–88, Mar. 2013.
[9] Q. M. Yue, F. P. Lu, W. Y. Yu, and J. Wang, "A novel algorithm to determine minimum break point set for optimum cooperation of directional protection relays in multiloop networks," *IEEE Trans. Power Del.*, vol. 21, no. 3, pp. 1114–1119, Jul. 2006.
[10] J. W. Yin, B. J. Ge, D. J. Tao, H. S. Zhao, and K. Yang, "Analysis of rotor eddy-current losses in large half speed turbo-generators under open-phase conditions," *J. Power Energy Syst.*, vol. 36, no. 20, pp. 5647–5656, Oct. 2016.
[11] H. Huang and X. Chu, "Improving rotational inertia of power system with variable speed synchronous condenser," in *Proc. IEEE Power Energy Soc. General Meeting, Chicago*, Feb. 2017, pp. 1–5.
[12] R. J. Dian, W. Xu, and C. X. Mu, "Improved negative sequence current detection and control strategy for H-bridge three-level active power filter," *IEEE Trans. Appl. Sup.*, vol. 26, no. 7, Oct. 2016, Art. no. 0611905.
[13] M. Breznik, V. Ambrožič, and M. Nemec, "Detection of open circuit fault in battery power supply feeding permanent magnet synchronous motor," *IET Power Electron.*, vol. 11, no. 14, pp. 2377–2384, Nov. 2018.
[14] U. Lahiri, A. K. Pradhan, and S. Mukhopadhyaya, "Modular neural network-based directional relay for transmission line protection," *IEEE Trans. Power Syst.*, vol. 20, no. 4, pp. 2154–2155, Nov. 2005.
[15] N. T. Stringer and D. Waser, "An innovative method of providing total breaker failure protection," *IEEE Trans. Ind. Appl.*, vol. 32, no. 5, pp. 1011–1016, Sep. 1996.
[16] T. M. Lindquist, L. Bertling, and R. Eriksson, "Circuit breaker failure data and reliability modelling," *IET Gener., Transmiss. Distrib.*, vol. 2, no. 6, pp. 813–820, Nov. 2008.
[17] G. Q. Li, *Transient Analysis of Power System*. Haikou, China: China Electric Power Press, 2007, pp. 136–146.
[18] W. J. Wang, *Power System Protective Relaying*, 2nd ed. Haikou, China: China Electric Power Press, 1998, pp. 45–68.
[19] B. T. Ooi and R. A. David, "Induction-generator/synchronous-condenser system for wind-turbine power," *Proc. Ins. Electr. Eng.*, vol. 126, no. 1, pp. 69–74, Jan. 1979.
[20] T. Petersson and K. Frank, "Starting of large synchronous motor using static frequency converter," *IEEE Trans. Power App. Syst.*, vol. 91, no. 1, pp. 172–179, Jan. 1972.

PUYU WANG (S'13–M'15) received the B.Eng. degree in electrical engineering from the Huazhong University of Science and Technology (HUST), China, and the University of Birmingham, U.K., in 2011, and the Ph.D. degree from the University of Birmingham, Birmingham, U.K., in 2016.

From 2013 to 2016, he was a Research Fellow in electrical power systems with the University of Birmingham. He is currently a Lecturer with the Department of Electrical Engineering, School of Automation, Nanjing University of Science & Technology (NUST), China. His research interests include HVDC technology, dc–dc converters, grid integration of renewable energy, and power electronics applications in power systems.

XING LIU is currently pursuing the M.Eng. degree in electrical engineering with the Nanjing University of Science & Technology (NUST), Nanjing, China.

His current research interests include start-up, protection & control of synchronous condenser, and HVDC technologies.

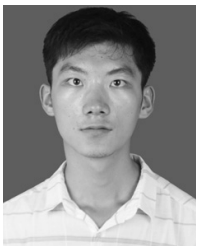

QINGWEN MOU received the B.Eng. degree in electrical engineering from the Nanjing University of Science & Technology (NUST), Nanjing, China, in 2018, where he is currently pursuing the M.Eng. degree in electrical engineering.

His research interests include operation, control and protection of synchronous condenser, and HVDC technologies.

WEI GU (M'06–SM'16) received the B.Sc. and Ph.D. degrees in electrical engineering from Southeast University, Nanjing, China, in 2001 and 2006, respectively.

From 2009 to 2010, he was a Visiting Scholar with the Department of Electrical Engineering, Arizona State University, Tempe, AZ, USA. He is currently a Professor with the School of Electrical Engineering, Southeast University. He is also the Director of the Institute of Distributed Generations and Active Distribution Networks. His research interests include distributed generations and microgrids, and active distribution networks.

YIDAN LIU received the B.Sc. degree in electrical engineering from Southeast University, Nanjing, China, in 2003. He is currently a Senior Engineer with Jiangsu Electric Power Maintenance Branch Company, China.

His research interests include relay protection, and operation & maintenance of synchronous condenser in power systems.